Sensors and Actuators B 166–167 (2012) 83–88

Contents lists available at SciVerse ScienceDirect

Sensors and Actuators B: Chemical

journal homepage: www.elsevier.com/locate/snb

Highly efficient rapid ethanol sensing based on $In_{2-x}Ni_xO_3$ nanofibers

Caihui Feng[a], Wei Li[a], Chao Li[a], Linghui Zhu[a], Haifeng Zhang[a], Ying Zhang[a], Shengping Ruan[a,*], Weiyou Chen[b,*], Lianxiang Yu[c,*]

[a] State Key Laboratory on Integrated Optoelectronics, Jilin University, Changchun 130012, PR China
[b] College of Electronic Science and Engineering, Jilin University, Changchun 130012, PR China
[c] College of Chemistry, Jilin University, Changchun 130012, PR China

ARTICLE INFO

Article history:
Received 4 October 2011
Received in revised form
16 December 2011
Accepted 23 December 2011
Available online 8 March 2012

Keywords:
NiO
In_2O_3
Ethanol sensors
Nanofibers
Electrospinning

ABSTRACT

Stable solid solution $In_{2-x}Ni_xO_3$ nanofibers were formed by introducing p-type NiO into n-type In_2O_3 via an electrospinning technique with a subsequent calcination process. The nanofibers were characterized by differential thermal and thermal gravimetric analyzer (DTA–TGA), scanning electron microscopy (SEM), X-ray diffraction (XRD), and X-ray photoelectron spectroscopy (XPS). Ethanol sensing properties of the as-prepared nanofibers were investigated in detail. In order to maintain the nanofibers' one-dimensional morphologies in the sensor fabrication, a unique measurement technique was introduced for the first time. The result showed that $In_{2-x}Ni_xO_3$ nanofibers exhibited significantly enhanced sensitivity, good selectivity, fast response and recovery rate (<3 s and <2 s), and excellent linearity in a relatively wide range of 1–500 ppm at a low temperature of 180 °C. These properties make the fabricated nanofibers good candidates for ethanol detection.

1. Introduction

Since their introduction in 1922 [1], chemical sensors have been extensively applied in the fields of air-quality control, environmental monitoring, healthcare, defense, security, etc. [2–5]. The past few decades have seen that the development of a wealth of simple, robust, solid-state sensors is closely related to both species and morphologies of the sensing materials. With the rapid and continuous development of nanoscience and technology, sensors based on one-dimensional (1D) nanostructure metal oxides semiconductor (MOS) (in the forms of fibers, wires, rods, belts, spirals, rings, tubes, etc.) have been stimulated and facilitated by the convenience of a rich variety of synthesis routes available (such as vapor–solid (VS), electrospinning, hydrothermal synthesis, and solvothermal routes) [6–9]. And the reports on corresponding sensors grow exponentially every year. In comparison with their bulk or zero dimension counterparts, the 1D nanomaterials have large surface area-to-volume ratios (a large surface area-to-volume ratio means that a significant fraction of the atoms (or molecules) are surface atoms that can participate in surface reactions) [10] and the congruence of the carrier screening length with their lateral dimensions will make them highly sensitive and efficient to transduce the surface chemical processes into electrical signals [11]. Therefore, they have been regarded as superior gas sensing candidates with versatile and outstanding performances. Among the various methods for generating 1D nanostructures, electrospinning (ES) emerged as a simple, efficient and versatile method for producing long continuous fibers with diameters ranging from several micrometers down to a few nanometers by applying a high voltage on a polymer solution or melt [12]; and developed rapidly in both academia and industry due to its several attractive features: comparatively low-cost, relatively high production rate, the ability to generate materials with large surface area-to-volume ratios, and applicability to many types of materials [13]. Up to now, ES has been employed to fabricate a wide variety of 1D nanostructure MOS like TiO_2 nanofibers, SnO_2 nanofibers, WO_3 nanowires, $SrTi_{1-x}Fe_xO_{3-\delta}$ nanofibers, and ZnO nanorods [14–18]. These MOS 1D nanomaterials have been fabricated into gas sensors which can mainly be divided into two types: one is the ceramic tube type on which a pair of Au electrodes was previously printed and Pt lead wires attaching to these electrodes were used as electrical contacts [19]; the other is the microsensor based on Si substrate [20]. However, in both kinds of the sensors, the 1D nanomaterials are usually pulverized to a pulp state and subsequently either directly painted or screen-printed in the sensor fabrication. This can more or less destroy the morphologies of the 1D nanomaterials and thus decrease their sensing properties correspondingly. Accordingly, developing a convenient and loss-less measurement technique to study the gas sensing properties of 1D nanomaterials is becoming a necessary and in urgent need.

* Corresponding authors. Tel.: +86 431 85168242; fax: +86 431 85168242.
E-mail addresses: rsp1226@gmail.com (S. Ruan), bjuqingqing@gmail.com (W. Chen), jluhuihui@gmail.com (L. Yu).

0925-4005/$ – see front matter © 2012 Elsevier B.V. All rights reserved.
doi:10.1016/j.snb.2011.12.083

MOS In_2O_3, with a direct bandgap of 3.55–3.75 eV, has been widely used as gas sensing materials to detect gases such as ethanol, H_2S, NO_2, NH_3, CO, and H_2 [21–26], due to its low resistance, good catalysis, strong interaction with the poisonous gas molecules, high sensitivity and large number of detectable gases [27,28]. For In_2O_3 nanostructures, many investigations have been focused on the sensing improvement by doping metal (Ag, Pt, Pd) [29–31] or metal oxide (SnO_2, ZnO, CeO_2) [32–34] in them. However, the reports on the In_2O_3-based solid-state solutions with 1D nanostructure have rarely been concerned. Solid solution materials are widely employed in catalyzer, oxygen storages/uptake capacity and chemical/physical sensors. The properties of these materials can be easily tailored by adjusting the rates of elements, and their selectivity and stability are also much better than normal metal oxides in gas sensors. Hitherto, solid solution materials such as SnO_2–TiO_2, ZrO_2–Fe_2O_3, ZnO–SnO_2, and SnO_2–MoO_3 have been proved to own outstanding sensing properties and thus been applied in practical sensor already [35–38]. Therefore, it can be hypothesized that In_2O_3-based solid-state solutions with 1D nanostructure may not only have some good sensing performances, but also provide some useful information for sensing enhancement.

In this paper, $In_{2-x}Ni_xO_3$ stable solid-state solution nanofibers were fabricated by introducing p-type NiO into n-type In_2O_3 via electrospinning and calcination techniques. Their ethanol sensing properties were investigated via a convenient and lossless measurement technique which was reported for the first time. Highly efficient sensing performance against ethanol was observed, which makes the fabricated nanomaterial a good candidate sensing material for high performance ethanol sensors.

2. Experimental

2.1. Chemical reagent

All the starting materials (AR grade): $In(NO_3)_3{\cdot}4.5H_2O$, $Ni(CH_3COO)_2{\cdot}4H_2O$, and polyvinyl pyrrolidone (PVP, Mw ≈ 1,300,000) were purchased from the Sinopharm Chemical Reagent Co. Ltd. and used as received without any further purification.

2.2. Preparation of the pure and Ni-doped In_2O_3 nanofibers

To prepare In_2O_3 and $In_{2-x}Ni_xO_3$ nanofibers, a certain amount of $In(NO_3)_3{\cdot}4.5H_2O$ and $Ni(CH_3COO)_2{\cdot}4H_2O$ powders were dissolved in 8.8 g mixed solution containing *N*,*N*-dimethylformamide (DMF)/ethanol (EtOH) with a weight ratio of 1:1 and stirred for 2 h. Then 0.8 g poly(vinyl pyrrolidone) (PVP, Mw ≈ 1,300,000) was added to the above solution with further stirring of 6 h. The obtained solution was then loaded into a plastic syringe and connected to a high-voltage power supply. A voltage of 20 kV was applied between the cathode (a flat aluminum foil) and the anode (syringe tip) at a distance of 20 cm. The precursor solution was directly electrospun on ceramic substrates with interdigitated Pd electrode arrays (finger spacing: 200 μm, finger depth: 20 μm). The as-spun composite fiber mats were then pressed with silica slides and calcined at 600 °C for 4 h in air. Finally after the removal of PVP, the precursor was transformed into polycrystalline nanofibers. All the measurements were carried out on the calcined nanofibers.

2.3. Measurement

The gas sensor (13.4 mm in length, 7 mm in width) shown in the inset of Fig. 1(a) was fabricated as follows: the composite nanofibers were firstly deposited on ceramic substrates with Ag–Pd electrodes, and then calcined together with the electrodes at 600 °C for 4 h on which a silicon slab was pressed on. The fabrication process is shown in Fig. 1(a).

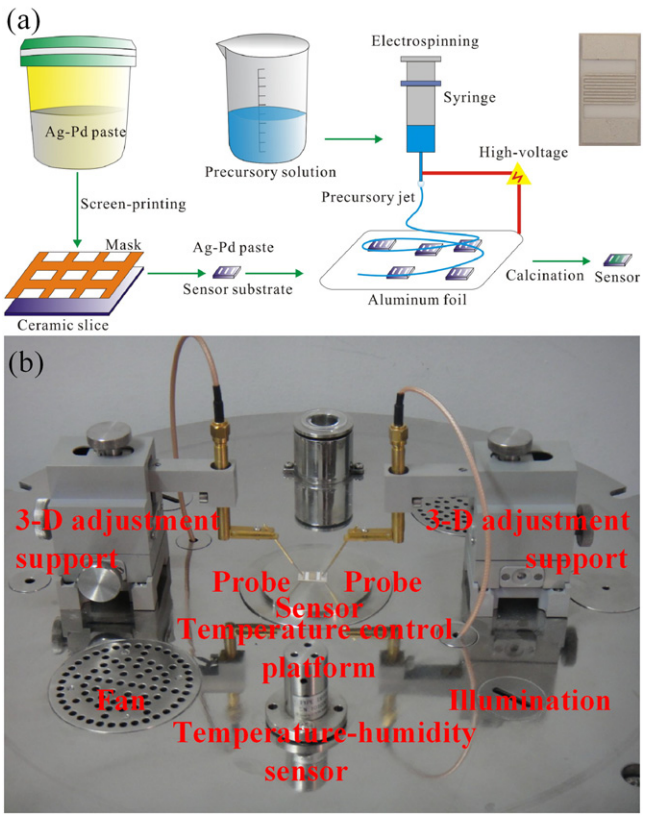

Fig. 1. Photographs of the sensor fabrication process (a) and obtained gas sensor (inset in (a)); and the gas-sensing analysis system (b).

The gas sensing properties of the sensor were measured by a CGS-1TP (Chemical Gas Sensor-1 Temperature Pressure) intelligent gas sensing analysis system (Beijing Elite Tech Co. Ltd., China). This multifunctional system shown in Fig. 1(b) consisted of the heating system, gas distribution system, probe adjustment system, vacuum system, measurement and data acquisition system, and measurement control software. The CGS-1TP analysis system offered an external temperature control (from room temperature to about 500 °C with a precision of 1 °C), which could conductively adjust the sensor temperature directly. Two probes were pressed on sensor substrates to export electrical signals. All the sensors were pre-heated at different operating temperatures for about 30 min. When the resistances of the sensors were stable, saturated target gas was injected into the test chamber (18 L in volume) by a microinjector through a rubber plug. The saturated target gas was mixed with air by two fans in the analysis system. After the sensor resistances reached new constant values, the test chamber was opened to recover the sensors in air. The whole experimental process was performed in a super-clean room with the constant humidity (25% relative humidity) and temperature (20 °C) (which were also monitored by the analysis system). The operating temperature of the sensors was reported by the analysis system automatically.

The response value (R) was designated as $R = R_a/R_g$, where R_a was the sensor resistance in air (base resistance) and R_g was that in a mixture of target gas and air. The time taken by the sensor resistance to change from R_a to $R_a - 90\% \times (R_a - R_g)$ was defined as response time when the target gas was introduced to the sensor, and the time taken from R_g to $R_g + 90\% \times (R_a - R_g)$ was defined as recovery time when the ambience was replaced by air.

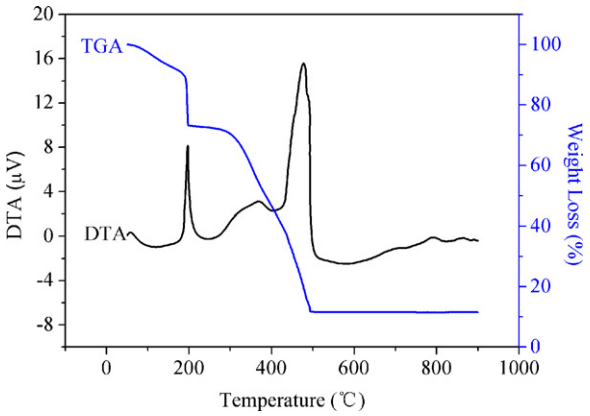

Fig. 2. DTA–TGA curves of the In $(NO_3)_3$/PVP/Ni$(CH_3COO)_2$ composite nanofibers.

2.4. Characterization

The nanofibers were characterized by differential thermal analyzer (DTA) and thermal gravimetric analyzer (TGA) (Melttler Toledo 825e); X-ray diffractometer (XRD) (Shimadzu XRD-6000, Cu Kα radiation); scanning electron microscopy (SEM) (XL30 ESEM FEG); and X-ray photoelectron spectrometer (XPS) (VG ESCA LAB MKII, Mg Kα radiation).

3. Results and discussion

3.1. Nanofiber characterization

The DTA–TGA curves of the In$(NO_3)_3$/PVP/Ni$(CH_3COO)_2$ composite nanofibers are displayed in Fig. 2. It is clear from the TGA curve that all the volatiles (H_2O and ethanol), organic components (PVP, DMF), CH_3COO^- and NO_3^- groups were removed completely below 550 °C, which resulted in a metal oxide phase. Moreover, the DTA curve exhibits two obvious exothermic peaks at 196 and 477 °C respectively, corresponding to the weight loss of approximately 77.2% between 191.1 °C and 505.1 °C. This significant weight loss was attributed to the complete decomposition of In$(NO_3)_3$, Ni$(CH_3COO)_2$ and the degradation of PVP, which involves both intra- and intermolecular transfer reactions [39]. And the minor weight loss before 191.1 °C corresponds to the removal of the free solvent in the precursors. According to the DTA–TGA analyses above, the following sintering temperature is chosen at 600 °C.

The XRD patterns of In_2O_3 and $In_{2-x}Ni_xO_3$ nanofibers calcined at 600 °C are shown in Fig. 3(a). All the diffraction peaks can be readily indexed to the cubic phase indium oxide (JCPDS card no. 06-0416) [40]. As for the $In_{2-x}Ni_xO_3$ nanofibers, there were no peaks corresponding to the nickel oxide or nickel, indicating that Ni element were effectively inserted into the crystal In_2O_3 lattice and formed stable $In_{2-x}Ni_xO_3$ substitution solid solution. Moreover it can be seen that the diffraction peaks of the $In_{2-x}Ni_xO_3$ nanofibers slightly shift to higher angles compared with that of In_2O_3 nanofibers. Detailed calculations showed that the lattice parameter decreased from 10.08940 Å to 10.05241 Å for transferring In_2O_3 nanofibers into $In_{2-x}Ni_xO_3$ nanofibers, respectively [41]. Considering the decrease of the unit cell constant, and that the ion radius of In^{3+} (0.72 Å) is between Ni^{2+} (0.78 Å) and Ni^{3+} (0.56 Å), we defer that there is an existence of ion Ni^{3+}, which may resulted from the partial electron change process as the following Eq. (1). Our assumption was further confirmed by the following XPS result in Fig. 3(b).

$$Ni^{2+} + In^{3+} \rightarrow Ni^{3+} + In^{2+} \quad (1)$$

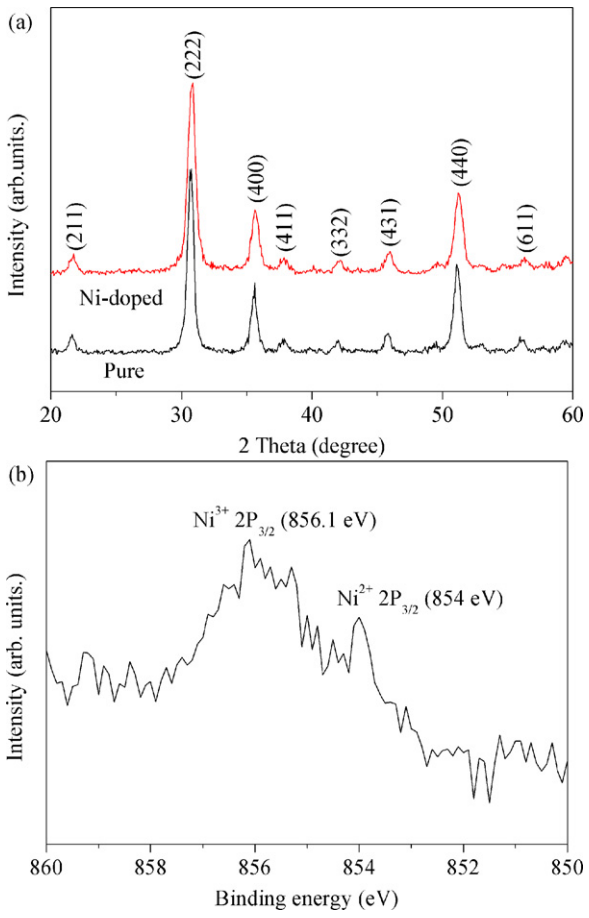

Fig. 3. (a) XRD patterns of In_2O_3 and $In_{2-x}Ni_xO_3$ nanofibers and (b) XPS patterns of the $In_{2-x}Ni_xO_3$ nanofibers.

To further confirm the presence of Ni^{3+} in the nanofibers, XPS measurements are carried out and shown in Fig. 3(b). The two peaks at Fig. 3(b) with binding energies of 854 eV and 856.1 eV correspond to Ni^{3+} $2P_{3/2}$ and Ni^{2+} $2P_{3/2}$ respectively, which further indicates the existence of Ni^{3+} in the Ni-doped nanofibers [41,42].

The SEM images of the as-electrospun composite nanofibers before and after calcination are shown in Fig. 4(a)–(d). It can be seen that the prepared In $(NO_3)_3$/PVP and In$(NO_3)_3$/PVP/Ni$(CH_3COO)_2$ composite nanofibers were collected as randomly oriented structures in the form of nonwoven mats because of the bending instability associated with the spinning jet. Each individual nanofiber was smooth and uniform in cross section with average diameters of about 350 nm (In_2O_3), 450 nm ($In_{2-x}Ni_xO_3$) and lengths of several microns. The precursor fibers were then heated to 600 °C under a heating rate of 10 °C/min and kept there for 4 h in an air atmosphere. As shown in Fig. 4(b) and (d), the nanofibers shrink; become bend and rough; but remained as continuous structures with the removing of PVP. While the average diameter of these fibers, composing nanoparticles in diameters of 14.02 and 11.28 nm (estimated from the XRD peaks using the Scherrer formula) was reduced to about 90 (In_2O_3) and 70 nm ($In_{2-x}Ni_xO_3$) respectively. This size reduction of the fibers is due to the loss of PVP and the crystallization of In_2O_3.

3.2. Evaluation of gas-sensing performance

In order to determine the optimum operating temperature, the responses of In_2O_3 and $In_{2-x}Ni_xO_3$ nanofibers to 100 ppm ethanol vapor were measured continually at different operating

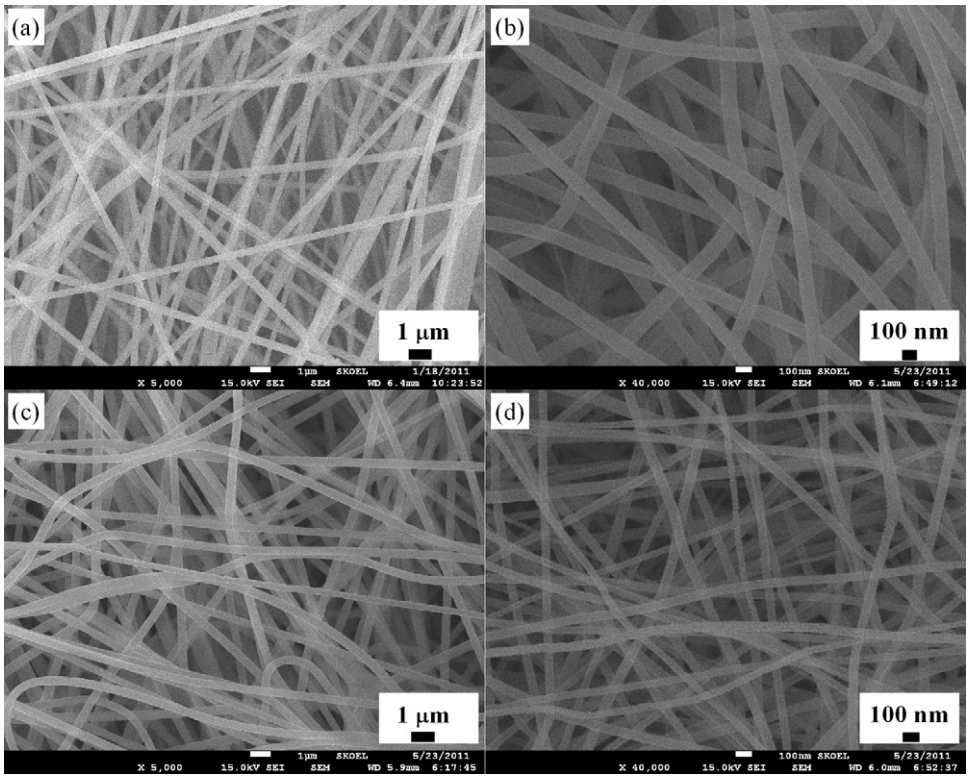

Fig. 4. SEM images of the In $(NO_3)_3$/PVP composite (a, b) and In$(NO_3)_3$/PVP/Ni$(CH_3COO)_2$ composite nanofibers: (a) and (c) before calcination; (b) and (d) after calcination.

temperatures (120–240 °C). As shown in Fig. 5, the responses of both sensors to ethanol vapor increased with the augment of operating temperatures and attained maximum values at about 180 °C, followed by a decrease with operating temperature. The temperature 180 °C was correspondingly identified as the optimum operating temperatures for both sensors and applied in all the investigations hereinafter. At this temperature, the $In_{2-x}Ni_xO_3$ nanofibers show significantly higher sensitivity than the pure samples with the maximum sensitivity of about 80 for 100 ppm ethanol vapor, indicating the addition of Ni is beneficial to In_2O_3 nanofibers for ethanol sensing.

The response of the $In_{2-x}Ni_xO_3$ nanofibers versus ethanol concentration at 180 °C is shown in Fig. 6. It can be easily found that the response increased rapidly with increasing of the ethanol concentration (1–500 ppm), and then gradually slowed down (500–5000 ppm), which indicated that the sensor becomes more or less saturated. Finally the sensor reached saturation at above 5000 ppm.

Moreover, the inset in Fig. 6 shows the linear calibration curve in the range of 1–500 ppm. Each data point with standard-deviation bars is obtained by measuring eight sensors. In fact, the response of the semiconducting oxide gas sensitive sensor can usually be empirically represented as $R = A[C]^N + B$, where A and B are constants and C is the concentration of the target gas. N usually has a value between 0.5 and 1.0, depending on the charge of the surface species and the stoichiometry of the elementary reactions on the surface [43]. For the $In_{2-x}Ni_xO_3$ nanofibers, N is around 1 for ethanol in the range of 1–500 ppm at 180 °C. The values of parameters A and B are 0.667 and 9.002 and their standard errors are 0.010 and 2.034, respectively. So the equation for the linear regression

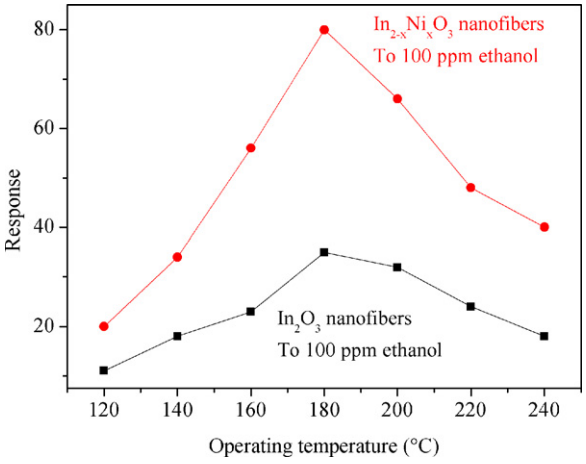

Fig. 5. Responses of In_2O_3 and $In_{2-x}Ni_xO_3$ nanofibers to 100 ppm ethanol vapor measured at different operating temperatures.

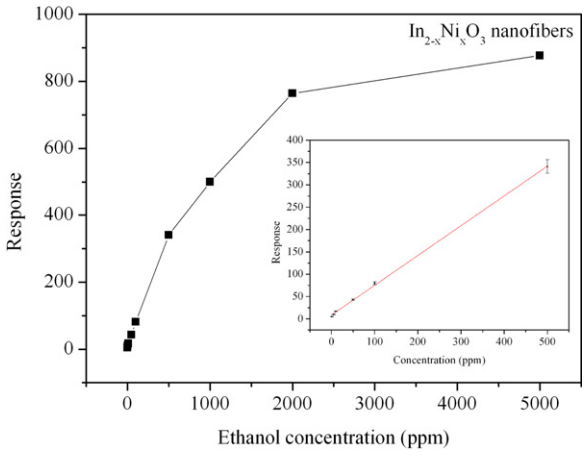

Fig. 6. The response of the $In_{2-x}Ni_xO_3$ nanofibers versus ethanol concentrations; the inset is the calibration curve in the range of 1–500 ppm.

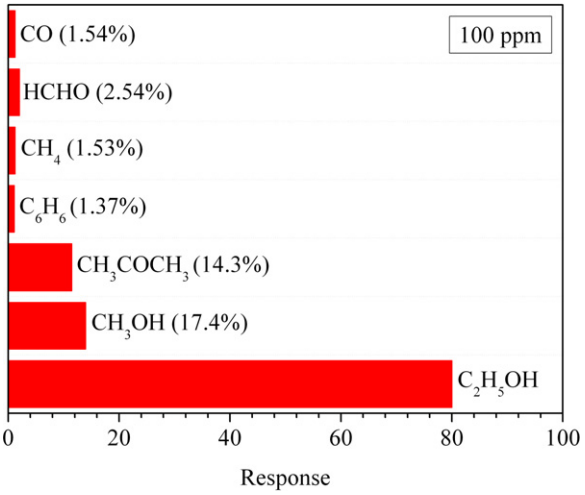

Fig. 7. Cross-responses of the $In_{2-x}Ni_xO_3$ nanofibers to 100 ppm different gases at 180 °C.

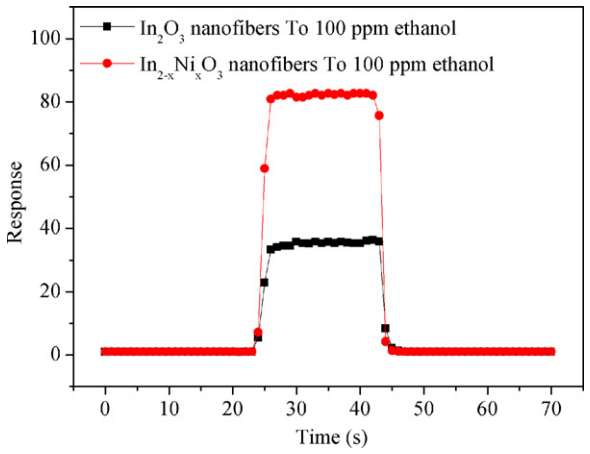

Fig. 8. Response and recovery behavior of In_2O_3 and $In_{2-x}Ni_xO_3$ nanofibers to 100 ppm ethanol at 180 °C.

can be simply expressed as $R = 0.667[C] + 9.002$. The detection limit of the $In_{2-x}Ni_xO_3$ nanofibers is about 1 ppm, and the corresponding response is about 5. This liner phenomenon between the sensitivity and the ethanol concentration was also observed in many reports. It is believed that the linear dependence of response on the ethanol concentration is related to the small size effect of nanomaterials. Such a linear dependence further shows that the nanofibers can be used as promising materials for ethanol sensors.

The gas sensing selectivity is another important parameter to evaluate the sensing ability of semiconductor materials. The cross-responses of the $In_{2-x}Ni_xO_3$ nanofibers to some typical VOCs gases such as CO, HCHO, CH_4, C_6H_6, CH_3COCH_3, and CH_3OH (the concentration of all these gases was 100 ppm) at 180 °C are shown in Fig. 7. As can be seen in this figure, the sensor exhibits much larger response to ethanol than to other VOC gases. The observed high sensitivity and selectivity of the $In_{2-x}Ni_xO_3$ nanofibers make the developed material suitable candidate for monitoring low concentrations of ethanol.

It is well known that the selectivity of the sensor is influenced by several factors, such as the lowest unoccupied molecule orbit (LUMO) energy of the gas molecule and the amount of gas adsorption on the sensing material at different operating temperatures. According to the previous reports, if the value of the LUMO energy becomes smaller, the energy needed for the gas sensing reaction will reduce and the sensing signal can be enhanced accordingly. The values of the LUMO energy for ethanol methanol acetone and formaldehyde are 0.12572 eV, 0.19728 eV, 0.20525 eV and 0.21965 eV, respectively, which means that the electrons transport more easily in ethanol molecules than in methanol, acetone and formaldehyde molecules to the conductance band of $In_{2-x}Ni_xO_3$ [21,44]. Therefore, the $In_{2-x}Ni_xO_3$ sensor shows higher sensitivity to ethanol than methanol acetone and formaldehyde.

As for gas sensing applications, rapid response and recovery are of great importance. Fig. 8 shows the response and recovery characteristics of In_2O_3 and $In_{2-x}Ni_xO_3$ nanofibers to 100 ppm ethanol at 180 °C. It can be seen that the response of the $In_{2-x}Ni_xO_3$ nanofiber is much higher than that of the pure nanofibers. Moreover, when the target gas was injected into the testing chamber the responses of both sensors increase rapidly; when subjected to air the sensor recovery to the initial state was also rapid. For In_2O_3 and $In_{2-x}Ni_xO_3$ nanofibers, the response time is less than 3 s and the recovery time is less than 2 s. The rapid response and recovery of the sensor can be attributed to the 1D nanostructure of our electrospun nanofibers, which can facilitate fast mass transfer of ethanol molecules to and from the interaction region as well as improve the rate for charge carriers to traverse the barriers introduced by molecular recognition events along the entire fibers [10].

The sensing mechanism can be explained as follows. The response of semi-conducting metal oxides is based on the reactions between gas molecule to be detected and the oxygen species on the surface of oxides. When $In_{2-x}Ni_xO_3$ nanofibers are surrounded by air, oxygen molecules can adsorb on their surface to generate chemisorbed oxygen species, which can lead to a decrease of fiber conductive. When the sensor is exposed to ethanol, ethanol molecules can react with the chemisorbed oxygen species and release the trapped electron back to the conduction band, which will increase the carrier concentration and electron mobility and result in the reducing of fiber resistance. The high sensitivity and quick response of the current nanofibers are related to their 1D nanostructure which can make the sensor absorb more ethanol molecules, and can also form web-like structure on sensor surface naturally. Simultaneously, the solid solution system can produce more vacant oxygen, leading more oxygen species absorbed on the surface of $In_{2-x}Ni_xO_3$ solid solution nanofibers, which eventually improve the sensing performances of $In_{2-x}Ni_xO_3$ nanofibers. Moreover, compared with other alternatives, no grinding or no spin-coating of the samples was needed in the sensor fabrication, which not only simplified the sensor fabrication process but also successfully maintained the fiber's morphologies and finally resulted in high sensing properties of the current sensors.

4. Conclusions

In summary, p-type NiO was introduced into n-type In_2O_3 and formed stable solid state $In_{2-x}Ni_xO_3$ solutions. Sensor based on In_2O_3 and $In_{2-x}Ni_xO_3$ nanofibers was fabricated and their ethanol sensing properties were measured in a convenient and lossless technique reported for the first time. The $In_{2-x}Ni_xO_3$ nanofibers exhibited a high sensitivity of about 80 for 100 ppm ethanol vapor, favorable selectivity, good linearity in the range of 1–500 ppm, fast response and recovery rate at the optimal operating temperature of 180 °C.

Acknowledgments

This research was financially supported by the National Natural Science Foundation of China (60977031, 61007022 and 61006013), Jilin Provincial Science and Technology Department (20060928). Chinese National Programs for High Technology Research and

Development (No. 2009AA03Z402), and Doctoral Found of Ministry of Education of China (20090061110040).

References

[1] M. Mascini, C. Cremisini, A new ph electrode for gas-sensing probes, Anal. Chim. Acta 92 (1977) 277–283.
[2] S. Maheshwari, H.-C. Chang, Assembly of multi-stranded nanofiber threads through AC electrospinning, Adv. Mater. 21 (2009) 349–354.
[3] X. Peng, Band gap and composition engineering on a nanocrystal (BCEN) in solution, Acc. Chem. Res. 43 (2010) 1387–1395.
[4] M.D. Regulacio, M.-Y. Han, Composition-tunable alloyed semiconductor nanocrystals, Acc. Chem. Res. 43 (2010) 621–630.
[5] D.D.D. Ma, C.S. Lee, F.C.K. Au, S.Y. Tong, S.T. Lee, Small-diameter silicon nanowire surfaces, Science 299 (2003) 1874–1877.
[6] Q. Qi, T. Zhang, L. Liu, X. Zheng, Synthesis and toluene sensing properties of SnO_2 nanofibers, Sens. Actuators B 137 (2009) 471–475.
[7] J. Xu, Y. Chen, J. Shen, Ethanol sensor based on hexagonal indium oxide nanorods prepared by solvothermal methods, Mater. Lett. 62 (2008) 1363–1365.
[8] X. Jiaqiang, C. Yuping, C. Daoyong, S. Jianian, Hydrothermal synthesis and gas sensing characters of ZnO nanorods, Sens. Actuators B 113 (2006) 526–531.
[9] N.S. Ramgir, I.S. Mulla, K.P. Vijayamohanan, A room temperature nitric oxide sensor actualized from Ru-doped SnO_2 nanowires, Sens. Actuators B 107 (2005) 708–715.
[10] A. Kolmakov, M. Moskovits, Chemical sensing and catalysis by one-dimensional metal-oxide nanostructures, Annu. Rev. Mater. Res. 34 (2004) 151–180.
[11] H. Yu, Z. Zhang, M. Han, X. Hao, F. Zhu, A general low-temperature route for large-scale fabrication of highly oriented ZnO nanorod/nanotube arrays, J. Am. Chem. Soc. 127 (2005) 2378–2379.
[12] B. Ding, M. Wang, X. Wang, J. Yu, G. Sun, Electrospun nanomaterials for ultrasensitive sensors, Mater. Today 13 (2010) 16–27.
[13] D. Yang, B. Lu, Y. Zhao, X. Jiang, Fabrication of aligned fibrous arrays by magnetic electrospinning, Adv. Mater. 19 (2007) 3702–3706.
[14] I.-D. Kim, A. Rothschild, B.H. Lee, D.Y. Kim, S.M. Jo, H.L. Tuller, Ultrasensitive chemiresistors based on electrospun TiO_2 nanofibers, Nano Lett. 6 (2006) 2009–2013.
[15] Y. Wang, I. Ramos, J.J. Santiago-Aviles, Detection of moisture and methanol gas using a single electrospun tin oxide nanofiber, IEEE Sens. J. 7 (2007) 1347–1348.
[16] G. Wang, Y. Ji, X. Huang, X. Yang, P.-I. Gouma, M. Dudley, Fabrication and characterization of polycrystalline WO_3 nanofibers and their application for ammonia sensing, J. Phys. Chem. B 110 (2006) 23777–23782.
[17] K. Sahner, P. Gouma, R. Moos, Electrodeposited and sol–gel precipitated p-type $SrTi_{1-x}Fe_xO_{3-\delta}$ semiconductors for gas sensing, Sensors 7 (2007) 1871–1886.
[18] M. Yang, T. Xie, L. Peng, Y. Zhao, D. Wang, Fabrication and photoelectric oxygen sensing characteristics of electrospun Co doped ZnO nanofibres, Appl. Phys. A 89 (2007) 427–430.
[19] C. Feng, S. Ruan, J. Li, B. Zou, J. Luo, W. Chen, W. Dong, F. Wu, Ethanol sensing properties of $LaCo_xFe_{1-x}O_3$ nanoparticles: effects of calcination temperature, co-doping, and carbon nanotube-treatment, Sens. Actuators B 155 (2011) 232–238.
[20] L. Li, Z. Tong, L. Shou-Chun, W. Lian-Yuan, F. Hui-Tao, L. Wei, In/Pd-doped SnO_2-based CO micro-structure sensor with high sensitivity and quick response, Chin. Phys. Lett. 26 (2009) 100702.
[21] Y. Li, J. Xu, J. Chao, D. Chen, S. Ouyang, J. Ye, G. Shen, High-aspect-ratio single-crystalline porous In_2O_3 nanobelts with enhanced gas sensing properties, J. Mater. Chem. 21 (2011) 12852.
[22] L. Xu, B. Dong, Y. Wang, X. Bai, Q. Liu, H. Song, Electrospinning preparation and room temperature gas sensing properties of porous In_2O_3 nanotubes and nanowires, Sens. Actuators B 147 (2010) 531–538.
[23] D. Zhang, Z. Liu, C. Li, T. Tang, X. Liu, S. Han, B. Lei, C. Zhou, Detection of NO_2 down to ppb levels using individual and multiple In_2O_3 nanowire devices, Nano Lett. 4 (2004) 1919–1924.
[24] N. Du, H. Zhang, B.D. Chen, X.Y. Ma, Z.H. Liu, J.B. Wu, D.R. Yang, Porous indium oxide nanotubes: layer-by-layer assembly on carbon-nanotube templates and application for room-temperature NH_3 gas sensors, Adv. Mater. 19 (2007) 1641–1645.
[25] A. Qurashi, E.M. El-Maghraby, T. Yamazaki, T. Kikuta, Catalyst supported growth of In_2O_3 nanostructures and their hydrogen gas sensing properties, Sens. Actuators B 147 (2010) 48–54.
[26] N. Singh, R.K. Gupta, P.S. Lee, Gold-nanoparticle-functionalized In_2O_3 nanowires as CO gas sensors with a significant enhancement in response, ACS Appl. Mater. Interfaces 3 (2011) 2246–2252.
[27] J. Xu, X. Wang, G. Wang, J. Han, Y.a. Sun, Solvothermal synthesis of In_2O_3 nanocrystal and its ethanol sensing mechanism, Electrochem. Solid-State Lett. 9 (2006) H103–H107.
[28] Z. Li, Y. Dzenis, Highly efficient rapid ethanol sensing based on Co-doped In_2O_3 nanowires, Talanta 85 (2011) 82–85.
[29] L. Liu, T. Zhang, S. Li, L. Wang, Y. Tian, Preparation, characterization, and gas-sensing properties of Pd-doped In_2O_3 nanofibers, Mater. Lett. 63 (2009) 1975–1977.
[30] J. Wang, B. Zou, S. Ruan, J. Zhao, Q. Chen, F. Wu, HCHO sensing properties of Ag-doped In_2O_3 nanofibers synthesized by electrospinning, Mater. Lett. 63 (2009) 1750–1753.
[31] W. Zheng, X. Lu, W. Wang, Z. Li, H. Zhang, Z. Wang, X. Xu, S. Li, C. Wang, Assembly of Pt nanoparticles on electrospun In_2O_3 nanofibers for H_2S detection, J. Colloid Interface Sci. 338 (2009) 366–370.
[32] D.-W. Kim, I.-S. Hwang, S.J. Kwon, H.-Y. Kang, K.-S. Park, Y.-J. Choi, K.-J. Choi, J.-G. Park, Highly conductive coaxial SnO_2–In_2O_3 heterostructured nanowires for Li ion battery electrodes, Nano Lett. 7 (2007) 3041–3045.
[33] C.-Y. Lin, Y.-Y. Fang, C.-W. Lin, J.J. Tunney, K.-C. Ho, Fabrication of NO_x gas sensors using In_2O_3–ZnO composite films, Sens. Actuators B 146 (2010) 28–34.
[34] L. Xu, H. Song, B. Dong, Y. Wang, J. Chen, X. Bai, Preparation and bifunctional gas sensing properties of porous In_2O_3–CeO_2 binary oxide nanotubes, Inorg. Chem. 49 (2010) 10590–10597.
[35] M. Radecka, K. Zakrzewska, M. Rkas, SnO_2–TiO_2 solid solutions for gas sensors, Sens. Actuators B 47 (1998) 194–204.
[36] G. Stefanic, B. Grzeta, K. Nomura, R. Trojko, S. Music, The influence of thermal treatment on phase development in ZrO_2–Fe_2O_3 and HfO_2–Fe_2O_3 systems, J. Alloys Compd. 327 (2001) 151–160.
[37] J. Haeng Yu, G. Man Choi, Electrical and CO gas sensing properties of ZnO–SnO_2 composites, Sens. Actuators B 52 (1998) 251–256.
[38] M. Ivanovskaya, E. Lutynskaya, P. Bogdanov, The influence of molybdenum on the properties of SnO_2 ceramic sensors, Sens. Actuators B 48 (1998) 387–391.
[39] Z. Li, Y. Fan, J. Zhan, In_2O_3 nanofibers and nanoribbons: preparation by electrospinning and their formaldehyde gas-sensing properties, Eur. J. Inorg. Chem. 2010 (2010) 3348–3353.
[40] P. Xu, Z. Cheng, Q. Pan, J. Xu, Q. Xiang, W. Yu, Y. Chu, High aspect ratio In_2O_3 nanowires: synthesis, mechanism and NO_2 gas-sensing properties, Sens. Actuators B 130 (2008) 802–808.
[41] M. Ivanovskaya, P. Bogdanov, Effect of NiII ions on the properties of In_2O_3-based ceramic sensors, Sens. Actuators B: Chem. 53 (1998) 44–53.
[42] N.V. Kosova, E.T. Devyatkina, V.V. Kaichev, Optimization of Ni^{2+}/Ni^{3+} ratio in layered $Li(Ni,Mn,Co)O_2$ cathodes for better electrochemistry, J. Power Sources 174 (2007) 965–969.
[43] Y.J. Chen, L. Nie, X.Y. Xue, Y.G. Wang, T.H. Wang, Linear ethanol sensing of SnO_2 nanorods with extremely high sensitivity, Appl. Phys. Lett. 88 (2006) 083105.
[44] Z. Wen, L. Tian-mo, Gas-sensing properties of SnO_2–TiO_2-based sensor for volatile organic compound gas and its sensing mechanism, Physica B: Condens. Matter 405 (2010) 1345–1348.

Biographies

Caihui Feng received the master degree in chemistry at Jilin University in 2009. She has been studying at the same university since 2010, and is mainly devoted to the research of functional nanomaterials and chemical sensors.

Wei Li received the bachelor degree in electronic science and engineering from Jilin University in 2010. He has been studying at the same university since 2010, and is mainly devoted to the research of functional nanomaterials and chemical sensors.

Chao Li received the bachelor degree in electronic science and engineering from Jilin University in 2011. He has been studying at the same university since 2011, and is mainly devoted to the research of functional nanomaterials and chemical sensors.

Haifeng Zhang received the master degree in electronic science and engineering from Jilin University in 2009. He has been studying at the same university since 2009, and is mainly devoted to the research of wide band gap semiconductor UV detectors.

Ying Zhang received the master degree in chemistry from Jilin University in 2011. She has been studying at the same university since 2011, and is mainly devoted to the research of functional nanomaterials and chemical sensors.

Shengping Ruan received the PhD degree of electronic science and engineering from Jilin University in 2001. Now, he is mainly devoted to the research of electronic functional materials and devices.

Weiyou Chen received the PhD degree of electronic science and engineering from Jilin University in 1992. Now, he is mainly devoted to the research of electronic functional materials and devices.

Lianxiang Yu received her bachelor degree of polymer function and materials from Jilin University in 1997. Now, she is mainly devoted to the research of functional nanomaterials.